ACS chemical biology

Articles

pubs.acs.org/acschemicalbiology

Targeting the r(CGG) Repeats That Cause FXTAS with Modularly Assembled Small Molecules and Oligonucleotides

Tuan Tran,[†,‡] Jessica L. Childs-Disney,[†] Biao Liu,[†,§] Lirui Guan,[†] Suzanne Rzuczek,[†] and Matthew D. Disney*[,†]

[†]Department of Chemistry, The Scripps Research Institute, Scripps Florida, 130 Scripps Way #3A1, Jupiter, Florida 33458, United States

[‡]Department of Chemistry, University at Buffalo, Buffalo, New York 14260, United States

Supporting Information

ABSTRACT: We designed small molecules that bind the structure of the RNA that causes fragile X-associated tremor ataxia syndrome (FXTAS), an incurable neuromuscular disease. FXTAS is caused by an expanded r(CGG) repeat (r(CGG)^{exp}) that inactivates a protein regulator of alternative pre-mRNA splicing. Our designed compounds modulate r(CGG)^{exp} toxicity in cellular models of FXTAS, and pull-down experiments confirm that they bind r(CGG)^{exp} *in vivo*. Importantly, compound binding does not affect translation of the downstream open reading frame (ORF). We compared molecular recognition properties of our optimal compound to oligonucleotides. Studies show that r(CGG)^{exp}'s self-structure is a significant energetic barrier for oligonucleotide binding. A fully modified 2′-OMethyl phosphorothioate is incapable of completely reversing an FXTAS-associated splicing defect and inhibits translation of the downstream ORF, which could have deleterious effects. Taken together, these studies suggest that a small molecule that recognizes structure may be more well suited for targeting highly structured RNAs that require strand invasion by a complementary oligonucleotide.

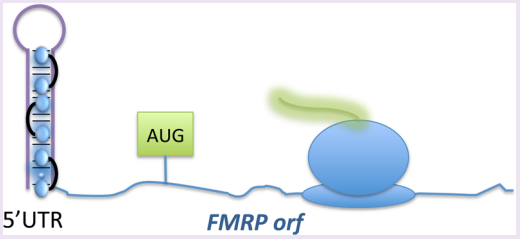

Oligonucleotides are the gold standard for targeting RNA as they have broad utility and can be designed using simple Watson−Crick base pairing rules.[1] Oligonucleotides, however, have several suboptimal properties as therapeutic modalities or chemical genetics probes of function, including poor cellular permeability and nonspecific stimulation of the immune system.[2−4] As an alternative to oligonucleotide-based therapeutics, we have been investigating RNA-small molecule interactions in an effort to establish design principles analogous to base pairing rules. In particular, we identify and characterize the preferred RNA secondary structural elements (motifs) of various small molecules.[5−7] Indeed, we have shown that these interactions can inform drug design.[8−11] That is, we compare the motifs within a cellular RNA to our set of RNA motif-small molecule interactions to identify lead small molecules. Lead small molecules can be optimized using various medicinal chemistry approaches such as definition of structure−activity relationships, structure-based design,[12−14] or chemical similarity searching.[15] Ideal RNA targets have more than one targetable motif, such that a multivalent compound can be designed to increase affinity and selectivity.[16−20]

Various diseases are caused by RNAs, including microsatellite disorders such as fragile X-associated tremor ataxia syndrome (FXTAS).[21] FXTAS is an incurable neurological disorder that is associated with multisystem atrophy, parkinsonism, dysautonomia, neuropathy, and dementia. The disease is caused via a gain-of-function by expanded r(CGG) repeats (r(CGG)^{exp})[22] located in the 5′ untranslated region (UTR) of the fragile X mental retardation 1 (*FMR1*) mRNA (encodes fragile X mental retardation protein; FMRP).[23−25] The repeat folds into a hairpin with an array of 1×1 nucleotide GG internal loops (Figure 1A).[9,22,26] The loops bind and sequester proteins involved in RNA biogenesis including DiGeorge syndrome critical region gene 8 protein (DGCR8), Src-associated in mitosis, 68 kDa protein (Sam68), and heterogeneous nuclear ribonucleoprotein (hnRNP).[22,26] Protein sequestration causes dysregulation of alternative pre-mRNA splicing in FXTAS model cellular systems and patient-derived tissue.[26] Although oligonucleotides have been employed successfully to improve defects associated with other microsatellite disorders,[27,28] they may not be ideal for r(CGG)^{exp} because it is highly structured and because depletion or inactivation of the *FMR1* mRNA via antisense or RNAi pathways could exacerbate disease; fragile X syndrome is caused by loss of FMRP.[29] Herein, we describe our studies to investigate the therapeutic potential of modularly assembled compounds and oligonucleotides that are complementary to r(CGG)^{exp} (Figure 1B). It is likely that certain types of RNAs are more suitable for small molecules while others are more suitable for oligonucleotides.

Received: November 26, 2013
Accepted: February 7, 2014
Published: February 7, 2014

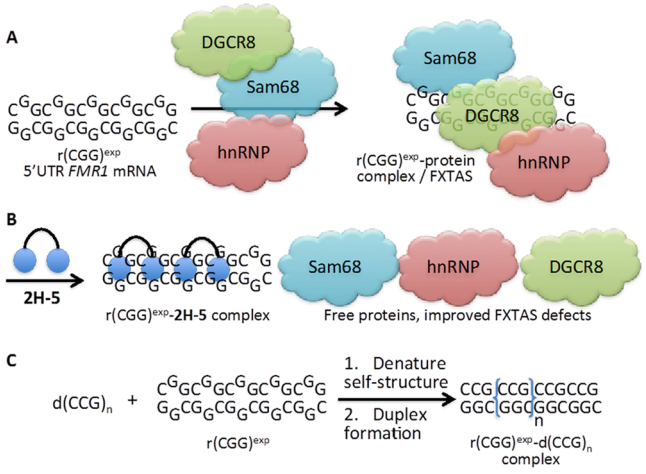

Figure 1. Disease pathology of FXTAS. (A) FXTAS is caused by r(CGG)^{exp} present in the 5′ UTR of the fragile X mental retardation 1 (*FMR1*) mRNA. The RNA folds into a hairpin with regularly repeating 1×1 nucleotide GG internal loops. The loops bind and sequester proteins that are involved in RNA biogenesis such as Sam68, hnRNP, and DGCR8. Formation of these r(CGG)^{exp}-protein complexes inactivates the proteins and causes FXTAS-associated defects in RNA biogenesis. (B) Designer small molecules targeting the repeating structure of r(CGG)^{exp} displace bound proteins, restoring their function. (C) Oligonucleotides complementary to r(CGG)^{exp} must disrupt the RNA's self-structure in order for duplex formation to occur, a significant energetic penalty that negatively affects potency.

RESULTS AND DISCUSSION

Design of Small Molecules That Bind r(CGG)^{exp}. In order to identify lead small molecules that bind r(CGG)^{exp}, the causative agent of FXTAS,[23−25] we compared its secondary structure to a set of RNA motif−small molecule interactions that have been identified and characterized by our laboratory.[5−7] In particular, we were interested in compounds that (i) bind to the repeating motifs in r(CGG)^{exp} (1×1 nucleotide GG internal loops; Figure 1) and (ii) can be modularly assembled to afford multivalent compounds that recognize the repeating structure of r(CGG)^{exp}, rather than a singular motif. Six small molecules including five aminoglycosides and the *bis*-benzimidazole **Ht-N$_3$**, which are well-known nucleic acid binders,[30,31] were identified as lead RNA-binding modules.[20] We chose **Ht-N$_3$** to pursue for further investigation because of its drug-like properties, cellular permeability in mammalian cells, and high affinity binding to 5′CGG/3′GGC (K_d = 375 ± 26 nM).[9] **Ht-N$_3$** also contains an orthogonal azide moiety that can be used for polyvalent display on a polymeric backbone (Figure 2B). A peptoid backbone was chosen as the modular display scaffold because (i) valency and the distance between RNA-binding modules can be easily controlled, (ii) their synthesis is facile and various RNA-binding modules can be easily incorporated,[32,33] and (iii) they are cell-permeable.[34]

In order to determine the distance between RNA-binding modules that most closely mimics the distance between 5′CGG/3′GGC motifs that periodically repeat in r(CGG)^{exp}, we screened a library of **H**-dimers[20] for disrupting a r(CGG)$_{12}$-protein complex *in vitro* (where **H** indicates the conjugated form **Ht-N$_3$**; Figure 2B). The following nomenclature is used for modularly assembled compounds: **2H-*n*** where **2H** indicates two **H** RNA-binding modules and ***n*** indicates the number of propylamine spacers (or distance) that separate **H**s (Figure 2B). The *in vitro* potencies of **Ht-N$_3$** and the library of dimers were measured using a previously reported time-resolved fluorescence resonance energy transfer (TR-FRET) assay (Table 1).[9] It has been previously shown that DGCR8 binds

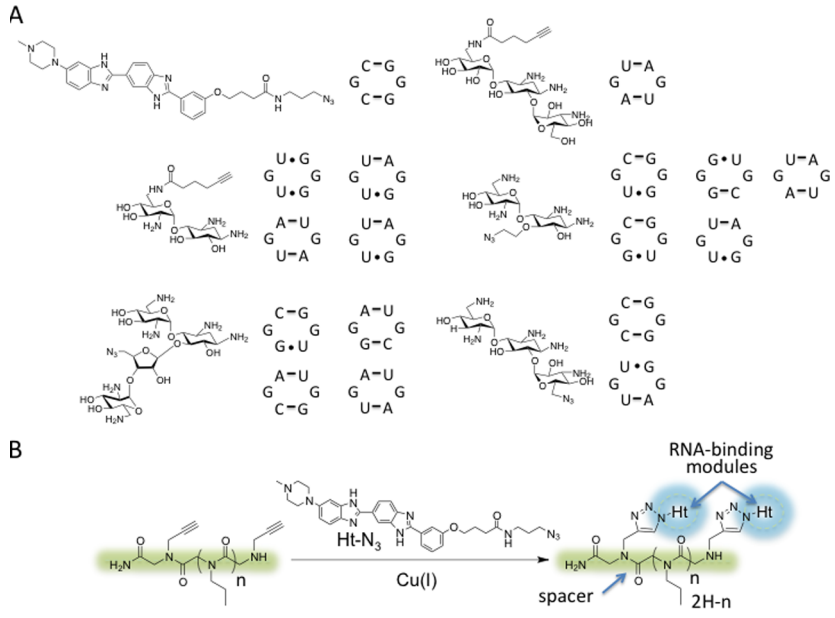

Figure 2. Lead compounds were identified by comparing the secondary structure of r(CGG)^{exp} to a database of RNA motif-small molecule interactions. One of the leads, **Ht-N$_3$**, was optimized using a modular assembly approach. **Ht-N$_3$** was selected for further investigation due to its drug-like properties and cellular permeability. (A) Structures of the lead compounds and their corresponding RNA motifs. (B) Structures of modularly assembled small molecules that target r(CGG)^{exp} using **Ht-N$_3$** as a lead small molecule. In order to develop multivalent compounds that target the repeating nature of r(CGG)^{exp}, the **Ht-N$_3$** module was anchored onto a peptoid scaffold. The distance between RNA-binding modules is controlled by the number of propylamine spacers conjugated between alkynes, which are used to conjugate **Ht-N$_3$** via a Cu(I)-catalyzed click reaction. The most potent compound most closely mimics the periodicity in r(CGG)^{exp} to inhibit protein binding.

dx.doi.org/10.1021/cb400875u | *ACS Chem. Biol.* 2014, 9, 904−912

Table 1. IC_{50}'s of Modularly Assembled Small Molecules for Inhibition of r(CGG)$_{12}$-DGCR8Δ Complexes *in Vitro* and *in Vivo*

compound	IC_{50} (μM)[a]	IC_{50} (μM) competitor[b]	% improvement of *SMN2* splicing[c]
Ht-N$_3$	33 ± 1	130 ± 4	2 ± 3
2H-1	18 ± 0.2	31 ± 2	4 ± 12
2H-2	17 ± 0.7	40 ± 4	11 ± 10
2H-3	18 ± 0.7	30 ± 0.7	30 ± 2
2H-4	20 ± 0.2	28 ± 1	25 ± 10
2H-5	18 ± 0.8	23 ± 3	34 ± 8
2H-6	23 ± 1	24 ± 2	27 ± 7
2H-7	35 ± 0.2	37 ± 1	33 ± 3

[a]IC_{50}'s were measured for disruption of a preformed RNA−protein complex. [b]Studies were completed in the presence of 65-fold excess tRNA over r(CGG)$_{12}$. [c]Compounds were tested at 20 μM concentration.

r(CGG)^{exp} and forms a scaffold for the binding of other proteins such as Sam68 and hnRNP.[9,26,35] Therefore, the TR-FRET assay measures the amount of r(CGG)$_{12}$-DGCR8Δ complex present.

Potencies and Affinities of Small Molecules. We completed IC_{50} measurements in the presence and absence of competitor tRNA (65-fold excess) (Table 1 and Supplementary Figure S-1). In the absence of competitor tRNA, **2H-1**−**2H-6** have similar potencies with IC_{50}'s ranging from 17 to 23 μM, an ∼1.6-fold increase in potency over monomer **Ht-N$_3$** (Table 1). In contrast, there is a wider range of IC_{50}'s in the presence of competitor tRNA, from 23 to 130 μM (Table 1). The most potent compounds are **2H-5** and **2H-6** with IC_{50}'s of 23 ± 1 and 24 ± 2 μM, respectively, which vary little from their IC_{50}'s in the absence of competitor and indicate that they are selective for r(CGG)$_{12}$. In contrast, the IC_{50} for **Ht-N$_3$** increases by ∼4-fold in the presence of competitor tRNA (33 ± 1 μM vs 130 ± 4 μM). Taken together, **2H-5** and **2H-6** are more selective than **Ht-N$_3$** (as evidenced by no change in their IC_{50}'s in the presence and absence of tRNA) and are ∼6-fold more potent than **Ht-N$_3$** in the presence of competitor (Table 1). The enhancement in potency is somewhat less than expected and may be due to a lack of preorganization of the modular assembly scaffold, which can be further optimized.

The affinity of **2H-5** for various RNAs was determined by using a fluorescence-based assay. **2H-5** forms a 1:1 complex (1.1 ± 0.2:1) with an RNA with one copy of the 5′CGG/3′CGG motif that periodically repeats in r(CGG)^{exp} (Supplementary Figure S-2) and binds with an affinity of 165 ± 5 nM. The affinity of the compound to an RNA with 12 copies of the 5′CGG/3′CGG motif (Supplementary Figure S-2) is enhanced by ∼3-fold (55 ± 10 nM). Moreover, **2H-5** occupies each 5′CGG/3′CGG binding site when statistical effects are taken into account as the stoichiometry is 4.6 ± 1.1:1 (**2H-5**:RNA).[36] The enhancement in affinity is not as large as expected, likely because the peptoid backbone has a great deal of conformational flexibility and thus is not preorganized for binding. Such effects have been previously observed.[16,20]

We studied the selectivity of **2H-5** *in vitro* by investigating its binding to r(CUG) repeats and bulk tRNA. Importantly, **2H-5** binds ∼5-fold more tightly to an RNA with 12 copies of a 5′CGG/3′CGG motif than to an RNA with 12 copies of a 5′CUG/3′CUG motif (K_d = 280 ± 76 nM; Supplementary Figure S-2). Moreover, **2H-5** binds weakly to competitor tRNA as no binding saturation was observed when up to 2 μM tRNA ($K_d \gg 2$ μM) was added (4-fold excess over **2H-5**), in agreement with IC_{50} values in the presence and absence of competitor tRNA, which do not change (Table 1). We previously reported that a similar compound, **2H-4**, is optimal for targeting 5′CUG/3′CUG repeats.[20] **2H-4** binds an RNA with 12 copies of a 5′CGG/3′CGG motif 4-fold more weakly than **2H-5** with a K_d of 212 ± 35 nM (Supplementary Figure S-2). Thus, the distance between RNA-binding modules contributes to the specificity of the small molecule.

In a previous report, we identified another small molecule, 9-hydroxy-5,11-dimethyl-2-(2-(piperidin-1-yl)ethyl)-6*H*-pyrido-[4,3-*b*]carbazol-2-ium (**1a**) by screening small molecule libraries for compounds similar to **Ht-N$_3$**.[9] **1a** binds r(CGG) repeats with high affinity (K_d = 76 ± 4 nM) and disrupts the binding of DGCR8Δ *in vitro* with an IC_{50} of 13 ± 0.4 μM.[9]

Potencies and Affinities of Oligonucleotides. Previous structural studies of r(CGG)^{exp} model systems have shown that the repeat forms a stable structure in which the 1×1 nucleotide GG internal loops adopt a *syn-anti* conformation with three hydrogen bonds.[37] Because of the stability of the loops and because r(CGG) repeats fold into an intramolecular hairpin (Supplementary Figure S-3), we hypothesized that the self-structure of the repeats poses a significant barrier for duplex formation with a complementary oligonucleotide. The significance of this barrier was probed using gel mobility shift assays in which r(CGG)$_{12}$ and a complementary oligonucleotide were folded either separately or together (Supplementary Figure S-4). These studies showed that the EC_{50} is 7-fold lower when oligonucleotides are folded with r(CGG)$_{12}$ than when they are folded separately (Supplementary Figure S-4). This large difference cannot be traced to oligonucleotide self-

Table 2. Oligonucleotide IC_{50}'s for Inhibition of a r(CGG)$_{12}$-DGCR8Δ Complex

	IC_{50} (μM)		
oligonucleotide	disruption	inhibition[b]	inhibition when oligo and RNA are folded together[c]
d(CCG)$_8$	>100[a]	50 ± 17	5 ± 1
d(CCG)$_{12}$	65 ± 6[a]	37 ± 2	1.6 ± 0.6
2′-OMe-PS-(CCG)$_{12}$	0.32 ± 0.04[a]	0.39 ± 0.02	0.16 ± 0.02
	0.57 ± 0.05 (5 min incubation)		
	0.35 ± 0.04 (30 min incubation)		
	0.32 ± 0.01 (45 min incubation)		

[a]Experiments were completed by disrupting a preformed r(CGG)$_{12}$-DGCR8Δ complex using the same conditions to collect the data in Table 1 including the presence of 65-fold excess of bulk tRNA. Samples were incubated for 60 min. [b]Oligonucleotides and r(CGG)$_{12}$ folded separately and then allowed to equilibrate prior to addition of DGCR8Δ. [c]Oligonucleotides and r(CGG)$_{12}$ were mixed together and folded by heating at 95 °C and slowly cooling to RT. DGCR8Δ was then added.

dx.doi.org/10.1021/cb400875u | *ACS Chem. Biol.* 2014, 9, 904−912

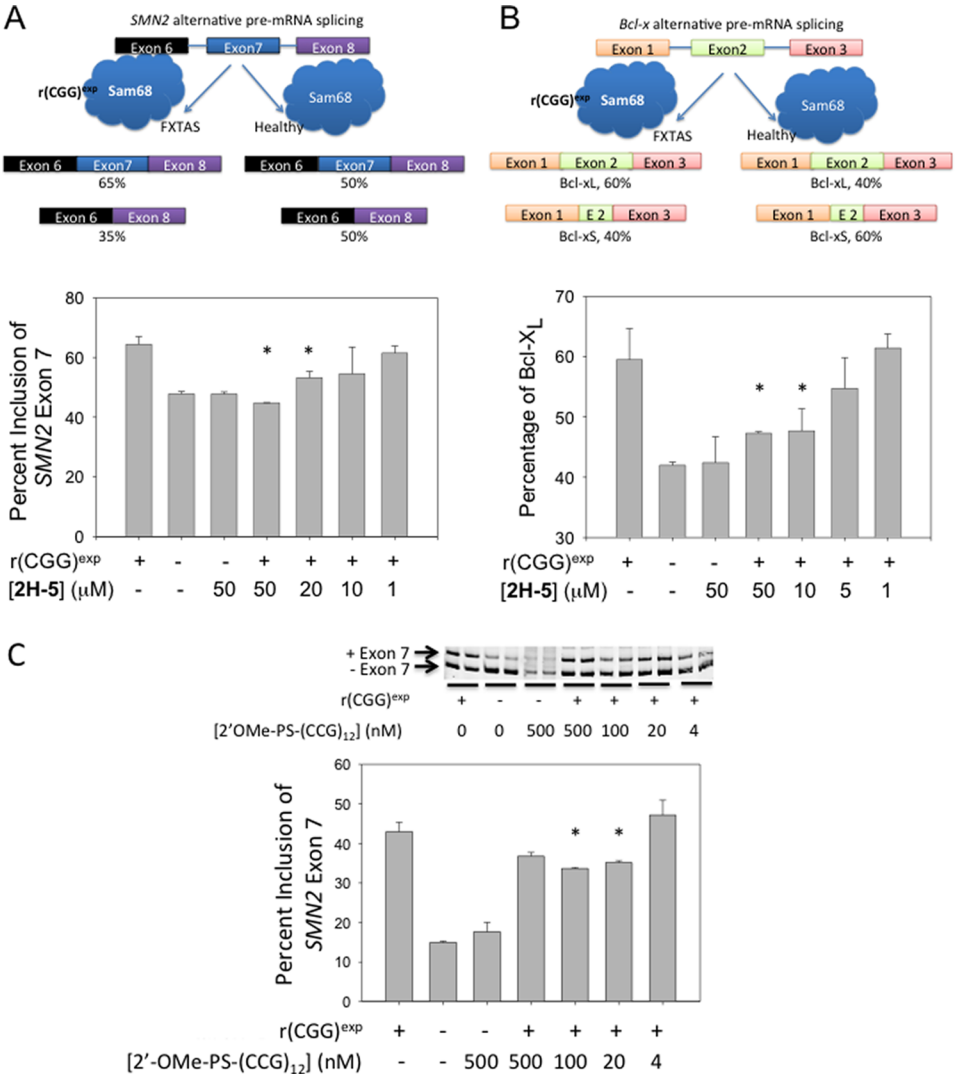

Figure 3. 2H-5 and 2′-OMe-PS-$(CCG)_{12}$ improve FXTAS-associated defects in alternative pre-mRNA splicing in a cell culture model. (A, top) Alternative splicing of *SMN2* pre-mRNA is regulated by Sam68.[19] When Sam68 is sequestered and inactivated by $r(CGG)^{exp}$, *SMN2* splicing is dysregulated. (A, bottom) When an FXTAS cell culture model is treated with **2H-5**, *SMN2* splicing patterns are restored as determined by RT-PCR. (B, top) Alternative splicing of *Bcl-x* pre-mRNA is also regulated by Sam68 and hence dysregulated in FXTAS.[19] (B, bottom) When a FXTAS cell culture model is treated with **2H-5**, normal *Bcl-x* splicing patterns are restored as determined by RT-PCR. (C) 2′OMe-PS-$(CCG)_{12}$ improves the *SMN2* pre-mRNA splicing defect when transfected into an FXTAS model system. Complete reversal of the splicing defect is not observed, however, even when cells are treated with 500 nM oligonucleotide. * denotes $p < 0.05$ as determined by a two-tailed Student's t test ($n \geq 2$). Error bars indicate standard deviation.

structure as both $d(CCG)_8$ and $d(CCG)_{12}$ form weak hairpin structures (as determined by optical melting experiments; $\Delta G^\circ_{37} \approx -1.5$ kcal/mol), but rather to the inherent stability of $r(CGG)_{12}$ ($\Delta G^\circ_{37} = -5.6$ kcal/mol) (Supplementary Figure S-3 and Supplementary Tables S1−S3). We predicted the contributions of the RNA's and oligonucleotide's self-structures to duplex formation using the OligoWalk program,[38] which confirmed that the self-structure of the RNA is a large energetic barrier (Supplementary Table S-4). (Please note that OligoWalk predicts duplex stability based on experimental measurements completed in 1 M Na^+, which is much different than conditions used herein (193 mM Na^+).)

The two DNA oligonucleotides were also studied for inhibition and disruption of the $r(CGG)_{12}$-DGCR8Δ complex (Table 2 and Supplementary Figure S-5). In the first set of experiments, the oligonucleotide and $r(CGG)_{12}$ were folded separately, mixed together, and incubated for 15 min prior to addition of DGCR8Δ. Under these conditions, $d(CGG)_{12}$ is only slightly more potent than $d(CGG)_8$, with IC_{50}'s of 37 and 50 μM, respectively. In the second set of experiments, the oligonucleotide and $r(CGG)_{12}$ were folded together and incubated for 15 min prior to addition of DGCR8Δ. Not unexpectedly, the IC_{50}'s of both compounds improve at least 10-fold, indicating that the self-structure of $r(CGG)_{12}$ significantly decreases oligonucleotide potency (Table 2).

Lastly, the $d(CCG)_n$ oligonucleotides were studied for disrupting a preformed $r(CGG)_{12}$-DGCR8Δ complex in the presence of competitor tRNA, the same conditions under which the IC_{50}'s for **2H-*n*** compounds were measured (Table 2). Not unexpectedly, $d(CCG)_{12}$ and $d(CCG)_8$ are poor inhibitors of the preformed complex, with IC_{50}'s of 65 and >100 μM, respectively (Table 2). (It should be noted that $d(CCG)_{12}$ and $d(CCG)_8$ do not bind DGCR8Δ as determined by gel mobility shift assays.)

dx.doi.org/10.1021/cb400875u | *ACS Chem. Biol.* 2014, 9, 904−912

Various studies have shown that the thermodynamic stability and other properties of complementary oligonucleotides can be improved by base and sugar modifications,[39] which could provide more potent modalities. For example, RNA-RNA duplexes are more thermodynamically stable than DNA-RNA duplexes;[40,41] 2′-OMe modification increases the thermodynamic stability of the resulting duplex by ∼0.1 kcal/mol per substitution,[42] and locked nucleic acids (LNAs) provide even greater enhancements.[43] In our case, we used a 2′-OMe oligonucleotide modified with a phosphorothioate (PS) backbone, or 2′-OMe-PS-$(CCG)_{12}$. Phosphorothioates have been well studied.[44] Although they decrease duplex stability[45,46] and selectivity in some cases,[44] they are resistant to nuclease cleavage, thereby increasing metabolic stability, and are generally nontoxic to animals.[47] Indeed, 2′-OMe-PS-$(CCG)_{12}$ is significantly more potent *in vitro* than $d(CCG)_{12}$ with an IC_{50} of ∼350 nM (Table 2).

Taken together, these studies establish that modularly assembled small molecules that target $r(CGG)^{exp}$ structure are more potent inhibitors of the $r(CGG)_{12}$-DGCR8Δ complex than DNA oligonucleotides that recognize sequence but less potent than an oligonucleotide with 2′-OMe modifications. Moreover, self-structure of the repeat is an impediment to complex formation with oligonucleotides.

Improvement of FXTAS-Associated Splicing Defects. Next, **Ht-N_3** and the **2H-*n*** compounds (20 μM) were screened for improving FXTAS-associated defects in a cell culture model (Table 1). The sequestration of Sam68 by $r(CGG)^{exp}$ (via DGCR8) causes dysregulation of alternative pre-mRNA splicing regulated by Sam68.[26] COS7 cells were co-transfected with a plasmid encoding $r(CGG)_{60X}$ and a survival of motor neuron 2 (*SMN2*) mini-gene, the alternative pre-mRNA splicing of which is regulated by Sam68.[26] The compound of interest was added in complete growth medium post-transfection, and alternative pre-mRNA splicing patterns were evaluated by RT-PCR. **2H-5** is the most potent, although similar improvements in *SMN2* splicing were observed with other compounds (Table 1).

The potency of **2H-5** *in vivo* was further characterized by completing a dose−response for improvement of *SMN2* and *Bcl-x* alternative splicing (also regulated by Sam68[26,48]) (Figure 3). The alternative pre-mRNA splicing patterns of both *SMN2* and *Bcl-x* are restored to wild type when cells are treated with 50 μM **2H-5**. Statistically significant improvement is observed for *SMN2* pre-mRNA at 20 μM dosage and for *Bcl-x* pre-mRNA at 10 μM dosage (as determined by comparing the percentage of exon inclusion in untreated cells that express $r(CGG)^{exp}$ to the percentage of exon inclusion in treated cells using a two-tailed Student's *t* test) (Figure 3). Importantly, **2H-5** does not affect the alternative splicing of the *SMN2* or *Bcl-x* pre-mRNAs in the absence of $r(CGG)_{60X}$ (Figure 3) or the alternative splicing of pre-mRNAs that are not regulated by Sam68 including cardiac troponin T (*cTNT*), insulin receptor (*IR*), or pleckstrin homology domain containing, family H member 2 (*PLEKHH2*) (Supplementary Figure S-6).[49−51] Interestingly, our previously reported compound, **1a**, improves FXTAS-associated pre-mRNA splicing defects, however it is ∼10-fold less potent than **2H-5** despite its higher affinity and potency *in vitro*.[9] This suggests that **1a** is either less selective *in vivo*, less cell-permeable, less metabolically stable, or some combination thereof compared with **2H-5**.

For comparison, we measured the *in vivo* potency of 2′-OMe-PS-$(CCG)_{12}$. A dose−response (4−500 nM) was completed in which the oligonucleotide was transfected into the FXTAS model cellular system. Somewhat surprisingly, no improvement was observed when cells were treated with 4 nM oligo. An improvement in splicing was observed when cells were transfected with 20 and 100 nM oligonucleotide (by ∼50% at 100 nM) (Figure 3C). Increasing the concentration of 2′-OMe-PS-$(CCG)_{12}$ to 500 nM, however, causes a slight reversion of the *SMN2* splicing defect. This is likely due to an off-target effect caused by the phosphorothioate backbone[52] as a scrambled oligonucleotide exacerbates splicing defects when cells are transfected with 100 and 500 nM oligo (but not 4 or 20 nM; Supplementary Figure S-7). Thus, in contrast to **2H-5**, 2′-OMe-PS-$(CCG)_{12}$ is incapable of completely reversing an FXTAS-associated splicing defect.

Effects on Translation of the Downstream ORF. Next, we evaluated if **2H-5** and 2′-OMe-PS-$(CCG)_{12}$ affect translation of the downstream open reading frame (ORF), which could be highly unfavorable. Fragile X syndrome is caused by loss of FMRP; thus, inhibiting translation of *FMR1* in FXTAS patients would likely worsen symptoms. For these studies, COS7 cells were transfected with a plasmid that encodes $r(CGG)_{88}$ in the 5′ UTR of GFP (in-frame). As shown in Figure 4, treatment with up to 20 μM **2H-5** does not affect the amount of GFP produced nor does it change the amount of transcript as determined by qRT-PCR. In contrast, 2′-OMe-PS-$(CCG)_{12}$ severely decreases translation of GFP (Figure 4A) and slightly increases the amount of $(CGG)_{88}$-GFP transcript (Figure 4B). These data suggest that 2′-OMe-PS-$(CCG)_{12}$ acts as a road block, impeding the translational machinery. Collectively, our *in vivo* studies suggest that oligonucleotides may not be ideal therapeutic modalities for FXTAS. 2′-OMe-PS-$(CCG)_{12}$ is incapable of restoring splicing patterns to wild type (Figure 3C), and even low nanomolar concentrations that have no effect on splicing outcomes significantly inhibit translation of the downstream ORF (50% inhibition at 4 nM; 90% inhibition at 100 nM) (Figure 4A). Since many oligonucleotide modifications are available,[39] it is possible that an oligonucleotide could be developed that improves splicing defects but does not inhibit translation of the downstream ORF. For example, peptide nucleic acids (PNAs) have been shown to possess enhanced strand invasion properties,[53] which will be particularly important for highly structured targets.

Oligonucleotides That Target Other Repeating RNAs. Oligonucleotides have been studied for reducing toxicity of other repeating RNAs, in particular $r(CUG)^{exp}$ (causative agent of myotonic dystrophy type 1; DM1) and $r(CAG)^{exp}$ (associated with Huntington's disease (HD) and spinocerebellar ataxia (SCA)). In general, they are more potent than oligonucleotides that target $r(CGG)^{exp}$ despite the fact that the oligonucleotides studied herein are much longer (36 nucleotides compared to 14−21 nucleotides). For example, (CAG)7, a fully phosphorothioate modified 2′-OMe oligonucleotide, silences transcripts containing $r(CUG)^{exp}$ with an IC_{50} of ∼0.4 nM.[27] Interestingly, a phosphorothioate DNA complementary to $r(CUG)^{exp}$ has an IC_{50} in cells of ∼300 nM (as measured by a 50% reduction in $r(CUG)^{exp}$ levels),[54] 1000-fold less potent than a phosphorothioate DNA-2′-OMe gapmer.[54] Other gapmers that are complementary to $r(CUG)^{exp}$ have similar potencies. An LNA-2′-*O*-methoxy ethyl (2′-MOE) gapmer significantly knocks down expression of $r(CUG)_{960}$ when cells are transfected with 0.3 nM oligonucleotide.[55] The gapmer also

dx.doi.org/10.1021/cb400875u | *ACS Chem. Biol.* 2014, 9, 904−912

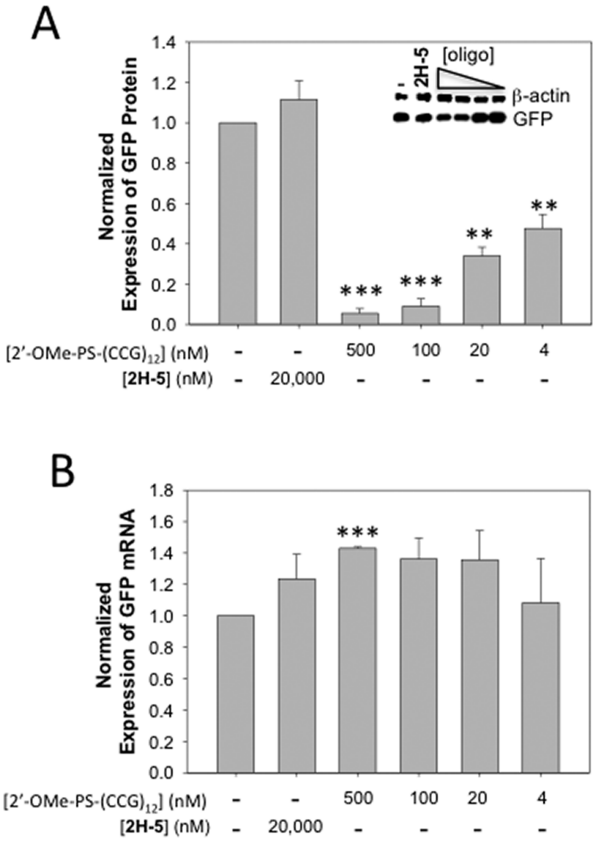

Figure 4. Binding of **2H-5** to r(CGG)^{exp} embedded in a 5′ UTR does not affect translation of a downstream open reading frame (ORF) (GFP). In contrast, binding of 2′-OMe-PS-$(CCG)_{12}$ inhibits translation, which could cause deleterious effects. (A) After treatment with **2H-5** or oligo, total protein was extracted and analyzed by Western blotting. Importantly, expression of the downstream ORF is unaffected by binding of **2H-5**. 2′-OMe-PS-$(CCG)_{12}$ inhibits translation even at 4 nM, a concentration that does not improve alternative splicing defects (Figure 3C). (B) We determined if **2H-5** and 2′-OMe-PS-$(CCG)_{12}$ affect mRNA expression levels by qRT-PCR. No change was observed for the compound or the oligonucleotide. This indicates that the decrease in GFP expression observed with treatment of 2′-OMe-PS-$(CCG)_{12}$ is due to impeding the translational machinery, not silencing of the transcript. ** denotes $p < 0.01$; *** indicates $p < 0.001$ as determined by a two-tailed Student's t test ($n = 2$). Error bars indicate standard deviation.

decreases $r(CUG)_{960}$ expression in a DM1 mouse model, significantly improving other DM1-associated defects.[55]

$(CUG)_7$, a 2′-OMe oligonucleotide complementary to r(CAG)^{exp} in mutant huntingtin (*HTT*) mRNA, was studied for allele-specific knock down of mutant HTT protein. $(CUG)_7$ has an IC_{50} for inhibition of mutant HTT protein expression between 2.5 and 5 nM in HD patient-derived cell lines, although it also affects expression of wild type HTT albeit to a lesser extent.[56] Four 19-nucleotide LNA-DNA gapmer complementary to r(CAG)^{exp} have IC_{50}'s between 27 and 40 nM.[57] Since 2′-OMe-PS-$(CCG)_{12}$ is significantly less potent than oligonucleotides that target other repeats, it suggests that the self-structure of r(CGG)^{exp} is a significant factor that should be considered in the development of oligonucleotide-based therapeutics.

Identification of the Cellular Targets of 2H-5 and d(CCG)$_{12}$. The nature of the modularly assembled compounds provides a unique opportunity to identify cellular targets. That is, the compounds can be easily modified to display a chemical handle for affinity-based purification. To identify the RNA targets of **2H-5**, we synthesized a **2H-5-biotin** derivative by coupling biotin carboxylate to the imino terminus of **2H-5** (Figure 5A, Supplementary Figures S-8 and S-9, and Supplementary Methods). **2H-5-Biotin** was then added to streptavidin resin to afford an affinity matrix. Likewise, we added **5′-biotin-d(CCG)$_{12}$** to streptavidin resin to identify the cellular RNA targets of the oligonucleotide.

Total RNA from a FXTAS model cellular system was applied to the affinity matrix displaying **2H-5** or the oligonucleotide. The resin was washed to remove unbound biomolecules, and the cellular targets were harvested and separated by gel electrophoresis. Although both **2H-5** and $d(CCG)_{12}$ bind r(CGG)^{exp} (confirmed by Northern blot; Supplementary Figure S-10), it appears that **2H-5** pulls down more of the target and that r(CGG)^{exp} comprises a larger percentage of all cellular targets as compared to $d(CCG)_{12}$ (Figure 5B and C). In order to confirm that these observations are indeed the case, we completed qRT-PCR of the pull-down with primers specific for r(CGG)^{exp} or 18S rRNA. There is 64-fold more r(CGG)^{exp} present in the RNAs pulled down by **2H-5** than by $d(CCG)_{12}$. Moreover, **2H-5** pulls down 16-fold more r(CGG)^{exp} than 18S rRNA, a 1.6-fold increase compared to the oligonucleotide. Taken together, this pull-down approach could be a general method that provides insight into the targets and off-targets of small molecules.

Summary and Conclusions. In summary, it is likely that different types of RNAs are more amenable to targeting by small molecules while other types are more amenable to targeting by oligonucleotides. Both classes of compounds show promise as therapeutic modalities that modulate the function of disease-associated RNAs. In the case of highly structured r(CGG)^{exp} residing in a 5′ UTR, we have shown that small molecule modalities may be better as they do not inhibit translation of the downstream ORF while also improving alternative pre-mRNA splicing defects.

METHODS

Synthesis of 2H-5-Biotin. Please see the Supporting Information for synthetic methods and compound characterization (Supplementary Figures S-8 and S-9).

Oligonucleotide Preparation and Purification. The RNA used in the protein displacement assay (5′-biotin-$r(CGG)_{12}$) was purchased from Dharmacon and deprotected per the manufacturer's recommended protocol. The RNA was desalted using a PD-10 gel filtration column (GE Healthcare). Concentration was determined by absorbance at 90 °C using a Beckman Coulter DU800 UV−vis spectrophotometer equipped with a Peltier temperature controller unit. The extinction coefficient (at 260 nm) was calculated using the HyTher server,[58] which uses nearest neighbors parameters.[59] DNA oligonucleotides were purchased from Integrated DNA Technologies (IDT) and used without further purification.

DGCR8Δ Expression and Purification. His-tagged DGCR8Δ was expressed and purified as previously described.[9]

Protein Displacement Assays. The protein displacement assay used to measure the IC_{50}'s of **2H-*n*** compounds and oligonucleotides inhibitors of the $r(CGG)_{12}$-DGCR8Δ complex was previously described ($n = 2$ for **2H-*n*** compounds; $n = 3$ for oligonucleotides).[9] The IC_{50}'s were determined by plotting percent inhibition of the $r(CGG)_{12}$-DGCR8Δ complex as a function of compound or oligonucleotide concentration. The resulting curves were fit to Sigma Plot's four parameter logistic curve fit.[9] Representative IC_{50} curves are provided in Supplementary Figures S-1 and S-5.

dx.doi.org/10.1021/cb400875u | ACS Chem. Biol. 2014, 9, 904−912

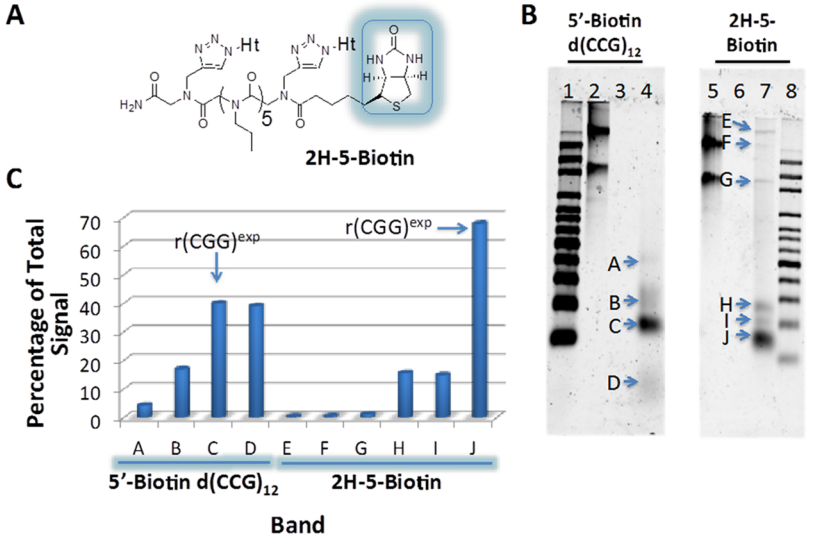

Figure 5. Identifying the cellular RNA targets of **2H-5-biotin** and **5′-Biotin-d(CCG)$_{12}$** via a pull-down assay. **2H-5-Biotin** and **5′-biotin-d(CCG)$_{12}$** were complexed with streptavidin-functionalized resin to afford an affinity matrix. (A) Structure of **2H-5-biotin**. (B) Representative gel image of the nucleic acids pull-downed by **2H-5-biotin** and **5′-biotin-d(CCG)$_{12}$**. Lanes: 1, DNA ladder; 2, total RNA isolated from an FXTAS cellular model system; 3, final wash of **5′-biotin-d(CCG)$_{12}$**-functionalized resin; 4, elution of RNA bound to **5′-biotin-d(CCG)$_{12}$**; 5, total RNA isolated from a FXTAS cellular model system; 6, final wash of **2H-5-biotin**-functionalized resin; 7, elution of RNAs bound to **2H-5-biotin**-functionalized resin; and 8, DNA ladder. (C) Quantitation of the gel image shown in B. Both **2H-5-biotin** and **5′-biotin-d(CCG)$_{12}$** recognize r(CGG)^{exp}. However, **2H-5-biotin** pulls down a larger amount of the target, which is also a larger percentage of the bound RNAs as confirmed by qRT-PCR.

Optical Melting Experiments. Optical melting experiments of 5′-biotin-r(CGG)$_{12}$, d(CCG)$_8$, and d(CCG)$_{12}$ were completed in 1X Melting Buffer (8 mM NaH_2PO_4, pH 7.0, 185 mM NaCl, and 1 mM EDTA) using a Beckman Coulter DU800 UV−vis spectrometer with an attached peltier heater. Melting curves of absorbance versus temperature were acquired at 260 nm with heating rate of 1 °C/min from 35 to 92 °C for r(CGG)$_{12}$ and 15 to 80 °C for d(CCG)$_8$ and d(CCG)$_{12}$. Melting curves were fit to a two-state model using the MeltWin program (http://www.meltwin.com) as previously described.[60] The results of optical melting experiments including normalized melting curves are provided in Supplementary Tables S-1−S-3 and Figure S-3.

Affinity Measurements. The affinities of **2H-5** and **2H-4** for various RNAs were determined as previously described (Supplementary Figure S-2).[20]

Treatment of a FXTAS Cell Culture Model with Small Molecules. In order to determine if **Ht-N$_3$** and **2H-*n*** compounds improve FXTAS-associated splicing defects *in vivo*, a cell culture model system was used as previously described.[9,26] Briefly, COS7 cells were maintained in growth medium (1X DMEM, 10% (v/v) FBS, and 1X GlutaMax (Invitrogen)). Cells were transfected using Lipofectamine 2000 reagent (Invitrogen) per the manufacturer's standard protocol using equal amounts of a plasmid expressing 60 CGG repeats ((CGG)$_{60X}$)[35] and a mini-gene of interest. Approximately 5 h post-transfection, the transfection cocktail was removed and replaced with growth medium containing 20 μM **Ht-N$_3$** or **2H-*n*** compound.

Treatment of an FXTAS Cell Culture Model with Oligonucleotides. COS7 cells were seeded in a 96-well plate and transfected with (CGG)$_{60X}$ and *SMN2* mini-genes as described above. Approximately 5 h post-transfection, cells were washed with 1X DPBS and transfected with oligonucleotide using Lipofectamine 2000 reagent in growth medium. Briefly, 25 μL of Opti-MEM containing oligonucleotide was mixed with 25 μL of Opti-MEM containing 1 μL of Lipofectamine 2000, and the samples were incubated for 20 min at room temperature. The mixture was then supplemented with 50 μL of 1X DMEM containing 20% (v/v) FBS and 2X GlutaMax and added to the cells. Cells were treated for 16−24 h followed by isolation of total RNA and/or protein.

Quantification of Alternative pre-mRNA Splicing by RT-PCR. RT-PCR amplification of alternative pre-mRNA splicing isoforms derived from mini-genes was completed as previously described.[9] Supplementary Table S-5 lists the RT-PCR primers used for each mini-gene construct. Splicing isoforms were separated using a 2−3% (w/v) agarose gel or a denaturing 5% (w/v) polyacrylamide gel stained with SYBR gold and quantified using QuantityOne software (BioRad). Statistical significance was determined by comparing splicing patterns in treated cells to untreated cells with a two-tailed Student's *t*-test ($n \geq 2$).

Western Blotting. After treatment, cells were lysed in the plate using 50 μL/well of M-PER Mammalian Protein Extraction Reagent containing 0.5 μL of Halt Protease Inhibitor cocktail (Thermo Scientific). A 5-μL aliquot of the cell lysate was boiled in 1X Laemmli Buffer. Cellular proteins were separated by SDS-PAGE and then transferred to PVDF membrane using a Trans-Blot Turbo Transfer System (Bio-Rad). Western blotting was completed using anti-GFP (Roche) or anti-β-actin (Sigma Aldrich) as primary antibodies and anti-IgG-horseradish peroxidase conjugate as the secondary antibody. Chemiluminescent signal was generated by adding 10 mL of SuperSignal West Pico Chemiluminescent substrate (Thermo Scientific), and the blot was imaged using Molecular Imager Gel Doc XR+ System (Bio-Rad). Statistical significance was determined by comparing the amount of GFP in treated cells to the amount in untreated cells using a two-tailed Student's *t*-test ($n = 2$).

qRT-PCR. Real time quantitative RT-PCR was completed to quantify the relative expression levels of 18S, β-actin, (CGG)$_{60X}$, or (CGG)$_{88}$-GFP as previously described.[61] Briefly, 400 ng of total RNA was reverse transcribed (25 μL total volume) to generate cDNA as previously described.[9] qPCR was completed in 10 μL using *Power* SYBR Green PCR Master Mix (Applied Biosystems) according to the manufacturer's protocol. PCR reactions contained 5 μL of 2X *Power* SYBR Green PCR Master Mix, 2 μL of the RT reaction, and 2 μM concentration of each primer. qPCR was perform on an ABI 7900 HT Real-Time PCR System (Applied Biosystems). The sequences of RT-PCR primers are provided in Supplementary Table S-5. Statistical significance was determined by comparing the amount of RNA of interest in treated cells to the amount of RNA of interest in untreated cells using a two-tailed Student's *t*-test ($n = 2$ biological replicates; $n = 3$ technical replicates).

dx.doi.org/10.1021/cb400875u | *ACS Chem. Biol.* 2014, 9, 904−912

■ ASSOCIATED CONTENT

Supporting Information

Synthetic methods, characterization of **2H-5-biotin**, methods for gel shift assays and Northern blotting, results of optical melting experiments, representative IC_{50} plots, representative gel images of gel mobility shift assays and RT-PCR analysis of alternative pre-mRNA splicing, and plots of controls for alternative splicing. This material is available free of charge via the Internet at http://pubs.acs.org.

■ AUTHOR INFORMATION

Corresponding Author

*E-mail: Disney@scripps.edu.

Present Address

[§]Center for Personalized Medicine, Roswell Park Cancer Institute, Buffalo, NY 14263.

Notes

The authors declare no competing financial interest.

■ ACKNOWLEDGMENTS

We thank P. Todd (University of Michigan, Department of Neurology) for the $(CGG)_{88}$-GFP construct. These studies were funded by the National Institutes of Health (R01-GM097455) and The Scripps Research Institute. M.D.D. is a Camille and Henry Dreyfus Teacher-Scholar.

■ REFERENCES

(1) Crooke, S. T. (2004) Progress in antisense technology. *Annu. Rev. Med. 55*, 61−95.

(2) Boggs, R. T., McGraw, K., Condon, T., Flournoy, S., Villiet, P., Bennett, C. F., and Monia, B. P. (1997) Characterization and modulation of immune stimulation by modified oligonucleotides. *Antisense Nucleic Acid Drug Dev. 7*, 461−471.

(3) Chan, J. H. P., Lim, S., and Wong, W. S. F. (2006) Antisense oligonucleotides: From design to therapeutic application. *Clin. Exp. Pharmacol. Physiol. 33*, 533−540.

(4) Galderisi, U., Cascino, A., and Giordano, A. (1999) Antisense oligonucleotides as therapeutic agents. *J. Cell. Physiol. 181*, 251−257.

(5) Disney, M. D., Labuda, L. P., Paul, D. J., Poplawski, S. G., Pushechnikov, A., Tran, T., Velagapudi, S. P., Wu, M., and Childs-Disney, J. L. (2008) Two-dimensional combinatorial screening identifies specific aminoglycoside-RNA internal loop partners. *J. Am. Chem. Soc. 130*, 11185−11194.

(6) Velagapudi, S. P., Pushechnikov, A., Labuda, L. P., French, J. M., and Disney, M. D. (2012) Probing a 2-aminobenzimidazole library for binding to RNA internal loops via two-dimensional combinatorial screening. *ACS Chem. Biol. 7*, 1902−1909.

(7) Velagapudi, S. P., Seedhouse, S. J., and Disney, M. D. (2010) Structure-activity relationships through sequencing (StARTS) defines optimal and suboptimal RNA motif targets for small molecules. *Angew. Chem., Int. Ed. 49*, 3816−3818.

(8) Childs-Disney, J. L., Hoskins, J., Rzuczek, S. G., Thornton, C. A., and Disney, M. D. (2012) Rationally designed small molecules targeting the RNA that causes myotonic dystrophy type 1 are potently bioactive. *ACS Chem. Biol. 7*, 856−862.

(9) Disney, M. D., Liu, B., Yang, W., Sellier, C., Tran, T., Charlet-Berguerand, N., and Childs-Disney, J. L. (2012) A small molecule that targets $r(CGG)^{exp}$ and improves defects in fragile X-associated tremor ataxia syndrome. *ACS Chem. Biol. 7*, 1711−1718.

(10) Kumar, A., Parkesh, R., Sznajder, L. J., Childs-Disney, J. L., Sobczak, K., and Disney, M. D. (2012) Chemical correction of pre-mRNA splicing defects associated with sequestration of muscleblind-like 1 protein by expanded r(CAG)-containing transcripts. *ACS Chem. Biol.* No. 7, 496−505.

(11) Parkesh, R., Childs-Disney, J. L., Nakamori, M., Kumar, A., Wang, E., Wang, T., Hoskins, J., Tran, T., Housman, D. E., Thornton, C. A., and Disney, M. D. (2012) Design of a bioactive small molecule that targets the myotonic dystrophy type 1 RNA via an RNA motif-ligand database and chemical similarity searching. *J. Am. Chem. Soc. 134*, 4731−4742.

(12) Stelzer, A. C., Frank, A. T., Kratz, J. D., Swanson, M. D., Gonzalez-Hernandez, M. J., Lee, J., Andricioaei, I., Markovitz, D. M., and Al-Hashimi, H. M. (2011) Discovery of selective bioactive small molecules by targeting an RNA dynamic ensemble. *Nat. Chem. Biol. 7*, 553−559.

(13) Davidson, A., Leeper, T. C., Athanassiou, Z., Patora-Komisarska, K., Karn, J., Robinson, J. A., and Varani, G. (2009) Simultaneous recognition of HIV-1 TAR RNA bulge and loop sequences by cyclic peptide mimics of Tat protein. *Proc. Natl. Acad. Sci. U.S.A. 106*, 11931−11936.

(14) Daldrop, P., Reyes, F. E., Robinson, D. A., Hammond, C. M., Lilley, D. M., Batey, R. T., and Brenk, R. (2011) Novel ligands for a purine riboswitch discovered by RNA-ligand docking. *Chem. Biol. 18*, 324−335.

(15) Willett, P. (2011) Similarity searching using 2D structural fingerprints. *Methods Mol. Biol. 672*, 133−158.

(16) Lee, M. M., Childs-Disney, J. L., Pushechnikov, A., French, J. M., Sobczak, K., Thornton, C. A., and Disney, M. D. (2009) Controlling the specificity of modularly assembled small molecules for RNA via ligand module spacing: targeting the RNAs that cause myotonic muscular dystrophy. *J. Am. Chem. Soc. 131*, 17464−17472.

(17) Kitov, P. I., Sadowska, J. M., Mulvey, G., Armstrong, G. D., Ling, H., Pannu, N. S., Read, R. J., and Bundle, D. R. (2000) Shiga-like toxins are neutralized by tailored multivalent carbohydrate ligands. *Nature 403*, 669−672.

(18) Mammen, M., Choi, S. K., and Whitesides, G. M. (1998) Polyvalent interactions in biological systems: Implications for design and use of multivalent ligands and inhibitors. *Angew. Chem., Int. Ed. 37*, 2755−2794.

(19) Arambula, J. F., Ramisetty, S. R., Baranger, A. M., and Zimmerman, S. C. (2009) A simple ligand that selectively targets CUG trinucleotide repeats and inhibits MBNL protein binding. *Proc. Natl. Acad. Sci. U.S.A. 106*, 16068−16073.

(20) Pushechnikov, A., Lee, M. M., Childs-Disney, J. L., Sobczak, K., French, J. M., Thornton, C. A., and Disney, M. D. (2009) Rational design of ligands targeting triplet repeating transcripts that cause RNA dominant disease: application to myotonic muscular dystrophy type 1 and spinocerebellar ataxia type 3. *J. Am. Chem. Soc. 131*, 9767−9779.

(21) Ranum, L. P., and Cooper, T. A. (2006) RNA-mediated neuromuscular disorders. *Annu. Rev. Neurosci. 29*, 259−277.

(22) Greco, C. M., Berman, R. F., Martin, R. M., Tassone, F., Schwartz, P. H., Chang, A., Trapp, B. D., Iwahashi, C., Brunberg, J., Grigsby, J., Hessl, D., Becker, E. J., Papazian, J., Leehey, M. A., Hagerman, R. J., and Hagerman, P. J. (2006) Neuropathology of fragile X-associated tremor/ataxia syndrome (FXTAS). *Brain 129*, 243−255.

(23) Brunberg, J. A., Jacquemont, S., Hagerman, R. J., Berry-Kravis, E. M., Grigsby, J., Leehey, M. A., Tassone, F., Brown, W. T., Greco, C. M., and Hagerman, P. J. (2002) Fragile X premutation carriers: characteristic MR imaging findings of adult male patients with progressive cerebellar and cognitive dysfunction. *Am. J. Neuroradiol. 23*, 1757−1766.

(24) Hagerman, R. J., Leehey, M., Heinrichs, W., Tassone, F., Wilson, R., Hills, J., Grigsby, J., Gage, B., and Hagerman, P. J. (2001) Intention tremor, parkinsonism, and generalized brain atrophy in male carriers of fragile X. *Neurology 57*, 127−130.

(25) Jacquemont, S., Hagerman, R. J., Leehey, M., Grigsby, J., Zhang, L., Brunberg, J. A., Greco, C., Des Portes, V., Jardini, T., Levine, R., Berry-Kravis, E., Brown, W. T., Schaeffer, S., Kissel, J., Tassone, F., and Hagerman, P. J. (2003) Fragile X premutation tremor/ataxia syndrome: molecular, clinical, and neuroimaging correlates. *Am. J. Hum. Genet. 72*, 869−878.

(26) Sellier, C., Rau, F., Liu, Y., Tassone, F., Hukema, R. K., Gattoni, R., Schneider, A., Richard, S., Willemsen, R., Elliott, D. J., Hagerman, P. J., and Charlet-Berguerand, N. (2010) Sam68 sequestration and partial loss of function are associated with splicing alterations in FXTAS patients. *EMBO J. 29*, 1248−1261.
(27) Mulders, S. A., van den Broek, W. J., Wheeler, T. M., Croes, H. J., van Kuik-Romeijn, P., de Kimpe, S. J., Furling, D., Platenburg, G. J., Gourdon, G., Thornton, C. A., Wieringa, B., and Wansink, D. G. (2009) Triplet-repeat oligonucleotide-mediated reversal of RNA toxicity in myotonic dystrophy. *Proc. Natl. Acad. Sci. U.S.A. 106*, 13915−13920.
(28) Wheeler, T. M., Sobczak, K., Lueck, J. D., Osborne, R. J., Lin, X., Dirksen, R. T., and Thornton, C. A. (2009) Reversal of RNA dominance by displacement of protein sequestered on triplet repeat RNA. *Science 325*, 336−339.
(29) Caplen, N. J., Parrish, S., Imani, F., Fire, A., and Morgan, R. A. (2001) Specific inhibition of gene expression by small double-stranded RNAs in invertebrate and vertebrate systems. *Proc. Natl. Acad. Sci. U.S.A. 98*, 9742−9747.
(30) Guan, L., and Disney, M. D. (2012) Recent advances in developing small molecules targeting RNA. *ACS Chem. Biol. 7*, 73−86.
(31) Thomas, J. R., and Hergenrother, P. J. (2008) Targeting RNA with small molecules. *Chem. Rev. 108*, 1171−1224.
(32) Simon, R. J., Kania, R. S., Zuckermann, R. N., Huebner, V. D., Jewell, D. A., Banville, S., Ng, S., Wang, L., Rosenberg, S., Marlowe, C. K., et al. (1992) Peptoids: a modular approach to drug discovery. *Proc. Natl. Acad. Sci. U.S.A. 89*, 9367−9371.
(33) Zuckermann, R. N., Kerr, J. M., Kent, S. B. H., and Moos, W. H. (1992) Efficient method for the preparation of peptoids [oligo(N-substituted glycines)] by submonomer solid-phase synthesis. *J. Am. Chem. Soc. 114*, 10646−10647.
(34) Kwon, Y. U., and Kodadek, T. (2007) Quantitative evaluation of the relative cell permeability of peptoids and peptides. *J. Am. Chem. Soc. 129*, 1508−1509.
(35) Sellier, C., Freyermuth, F., Tabet, R., Tran, T., He, F., Ruffenach, F., Alunni, V., Moine, H., Thibault, C., Page, A., Tassone, F., Willemsen, R., Disney, M. D., Todd, P. K., and Charlet-Berguerand, N. (2013) Sequestration of DROSHA and DGCR8 by expanded CGG-repeats RNA alters microRNA processing in fragile X-assoicated tremor/ataxia syndrome. *Cell Rep. 3*, 869−80.
(36) McGhee, J. D., and von Hippel, P. H. (1974) Theoretical aspects of DNA-protein interactions: co-operative and non-co-operative binding of large ligands to a one-dimensional homogeneous lattice. *J. Mol. Biol. 86*, 469−489.
(37) Kumar, A., Fang, P., Park, H., Guo, M., Nettles, K. W., and Disney, M. D. (2011) A crystal structure of a model of the repeating r(CGG) transcript found in Fragile X Syndrome. *ChemBioChem 12*, 2140−2142.
(38) Mathews, D. H., Burkard, M. E., Freier, S. M., Wyatt, J. R., and Turner, D. H. (1999) Predicting oligonucleotide affinity to nucleic acid targets. *RNA 5*, 1458−1469.
(39) Kurreck, J. (2003) Antisense technologies. Improvement through novel chemical modifications. *Eur. J. Biochem. 270*, 1628−1644.
(40) Sugimoto, N., Katoh, M., Nakano, S., Ohmichi, T., and Sasaki, M. (1994) RNA/DNA hybrid duplexes with identical nearest-neighbor base-pairs have identical stability. *FEBS Lett. 354*, 74−78.
(41) Sugimoto, N., Nakano, S., Katoh, M., Matsumura, A., Nakamuta, H., Ohmichi, T., Yoneyama, M., and Sasaki, M. (1995) Thermodynamic parameters to predict stability of RNA/DNA hybrid duplexes. *Biochemistry 34*, 11211−11216.
(42) Freier, S. M., and Altmann, K. H. (1997) The ups and downs of nucleic acid duplex stability: structure-stability studies on chemically-modified DNA:RNA duplexes. *Nucleic Acids Res. 25*, 4429−4443.
(43) Vester, B., and Wengel, J. (2004) LNA (locked nucleic acid): high-affinity targeting of complementary RNA and DNA. *Biochemistry 43*, 13233−13241.
(44) Agrawal, S. (1999) Importance of nucleotide sequence and chemical modifications of antisense oligonucleotides. *Biochim. Biophys. Acta 1489*, 53−68.
(45) Kibler-Herzog, L., Zon, G., Uznanski, B., Whittier, G., and Wilson, W. D. (1991) Duplex stabilities of phosphorothioate, methylphosphonate, and RNA analogs of two DNA 14-mers. *Nucleic Acids Res. 19*, 2979−2986.
(46) Stein, C. A., and Cheng, Y. C. (1993) Antisense oligonucleotides as therapeutic agents−is the bullet really magical? *Science 261*, 1004−1012.
(47) Swayze, E. E., and Bhat, B. (2008) The medicinal chemistry of oligonucleotides, in *Antisense Drug Technology: Principles, Strategies, and Applications* (Crooke, S. T., Ed.) 2nd ed., CRC Press, Boca Raton, FL.
(48) Paronetto, M. P., Achsel, T., Massiello, A., Chalfant, C. E., and Sette, C. (2007) The RNA-binding protein Sam68 modulates the alternative splicing of *Bcl-x*. *J. Cell. Biol. 176*, 929−939.
(49) Philips, A. V., Timchenko, L. T., and Cooper, T. A. (1998) Disruption of splicing regulated by a CUG-binding protein in myotonic dystrophy. *Science 280*, 737−741.
(50) Warf, M. B., Nakamori, M., Matthys, C. M., Thornton, C. A., and Berglund, J. A. (2009) Pentamidine reverses the splicing defects associated with myotonic dystrophy. *Proc. Natl. Acad. Sci. U.S.A. 106*, 18551−18556.
(51) Dansithong, W., Paul, S., Comai, L., and Reddy, S. (2005) MBNL1 is the primary determinant of focus formation and aberrant insulin receptor splicing in DM1. *J. Biol. Chem. 280*, 5773−5780.
(52) Stein, C. A. (1997) Controversies in the cellular pharmacology of oligodeoxynucleotides. *Ciba Found. Symp. 209*, 79−93.
(53) Smulevitch, S. V., Simmons, C. G., Norton, J. C., Wise, T. W., and Corey, D. R. (1996) Enhancement of strand invasion by oligonucleotides through manipulation of backbone charge. *Nat. Biotechnol. 14*, 1700−1704.
(54) Gonzalez-Barriga, A., Mulders, S. A., van de Giessen, J., Hooijer, J. D., Bijl, S., van Kessel, I. D., van Beers, J., van Deutekom, J. C., Fransen, J. A., Wieringa, B., and Wansink, D. G. (2013) Design and analysis of effects of triplet repeat oligonucleotides in cell models for myotonic dystrophy. *Mol. Ther. Nucleic Acids 2*, e81.
(55) Lee, J. E., Bennett, C. F., and Cooper, T. A. (2012) RNase H-mediated degradation of toxic RNA in myotonic dystrophy type 1. *Proc. Natl. Acad. Sci. U.S.A. 109*, 4221−4226.
(56) Evers, M. M., Pepers, B. A., van Deutekom, J. C., Mulders, S. A., den Dunnen, J. T., Aartsma-Rus, A., van Ommen, G. J., and van Roon-Mom, W. M. (2011) Targeting several CAG expansion diseases by a single antisense oligonucleotide. *PLoS One 6*, e24308.
(57) Gagnon, K. T., Pendergraff, H. M., Deleavey, G. F., Swayze, E. E., Potier, P., Randolph, J., Roesch, E. B., Chattopadhyaya, J., Damha, M. J., Bennett, C. F., Montaillier, C., Lemaitre, M., and Corey, D. R. (2010) Allele-selective inhibition of mutant huntingtin expression with antisense oligonucleotides targeting the expanded CAG repeat. *Biochemistry 49*, 10166−10178.
(58) SantaLucia, J., Jr. (1998) A unified view of polymer, dumbbell, and oligonucleotide DNA nearest-neighbor thermodynamics. *Proc. Natl. Acad. Sci. U.S.A. 95*, 1460−1465.
(59) Puglisi, J. D., and Tinoco, I., Jr. (1989) Absorbance melting curves of RNA. *Methods Enzymol 180*, 304−325.
(60) McDowell, J. A., and Turner, D. H. (1996) Investigation of the structural basis for thermodynamic stabilities of tandem GU mismatches: solution structure of $(rGAGGUCUC)_2$ by two-dimensional NMR and simulated annealing. *Biochemistry 35*, 14077−14089.
(61) Guan, L., and Disney, M. D. (2013) Small molecule-mediated cleavage of RNA in living cells. *Angew. Chem., Int. Ed. 52*, 1462−1465.